

A PALMPRINT RECOGNITION ALGORITHM USING PHASE-BASED IMAGE MATCHING

Koichi Ito[†], Takafumi Aoki[†], Hiroshi Nakajima[‡], Koji Kobayashi[‡] and Tatsuo Higuchi[§]

[†] Graduate School of Information Sciences, Tohoku University,
Sendai-shi 980-8579, Japan

E-mail: ito@aoki.ecei.tohoku.ac.jp

[‡] Yamatake Corporation, Isehara-shi 259-1195, Japan

[§] Faculty of Engineering, Tohoku Institute of Technology, Sendai-shi 982-8577, Japan

ABSTRACT

A major approach for palmprint recognition today is to extract feature vectors corresponding to individual palmprint images and to perform palmprint matching based on some distance metrics. One of the difficult problems in feature-based recognition is that the matching performance is significantly influenced by many parameters in feature extraction process, which may vary depending on environmental factors of image acquisition. This paper presents a palmprint recognition algorithm using phase-based image matching. The use of phase components in 2D (two-dimensional) discrete Fourier transforms of palmprint images makes possible to achieve highly robust palmprint recognition. Experimental evaluation using a palmprint image database clearly demonstrates an efficient matching performance of the proposed algorithm.

Index Terms— image processing, pattern recognition, security, identification of persons, image recognition, pattern matching

1. INTRODUCTION

Biometric authentication has been receiving much attention over the past decade with increasing demands in automated personal identification. Among many biometric techniques, palmprint recognition is one of the most reliable approaches, since a palmprint, the large inner surface of a hand, contains many features such as principle lines, ridges, minutiae points, singular points and texture [1].

A major approach for palmprint recognition today is to extract feature vectors corresponding to individual palmprint images and to perform palmprint matching based on some distance metrics [1, 2]. One of the difficult problems in feature-based palmprint recognition is that the matching performance is significantly influenced by many parameters in feature extraction process (e.g., spatial position, orientation, center frequencies and size parameters for 2D Gabor filter kernel), which may vary depending on environmental factors of palmprint image acquisition.

This paper presents an efficient algorithm for palmprint recognition using phase-based image matching — an image matching technique using the phase components in 2D Discrete Fourier Transforms (DFTs) of given images. The technique has been successfully applied to sub-pixel image registration tasks for computer vision applications [3, 4]. In our

previous work [5, 6, 7], we have proposed a fingerprint recognition algorithm using phase-based image matching, which has already been implemented in actual fingerprint verification units [8]. We also have proposed an iris recognition algorithm using phase-based image matching [9].

In this paper, we demonstrate that the same technique is also highly effective for palmprint recognition. The use of phase information makes possible to achieve highly robust palmprint recognition. Experimental evaluation using the PolyU palmprint database [10] clearly demonstrates an efficient matching performance of the proposed algorithm compared with a feature-based algorithm.

2. PHASE-BASED IMAGE MATCHING

In this section, we introduce the principle of phase-based image matching using the Phase-Only Correlation (POC) function (which is sometimes called the “phase-correlation function”) [3, 4, 11]. Consider two $N_1 \times N_2$ images, $f(n_1, n_2)$ and $g(n_1, n_2)$, where we assume that the index ranges are $n_1 = -M_1, \dots, M_1$ ($M_1 > 0$) and $n_2 = -M_2, \dots, M_2$ ($M_2 > 0$) for mathematical simplicity, and hence $N_1 = 2M_1 + 1$ and $N_2 = 2M_2 + 1$. Let $F(k_1, k_2)$ and $G(k_1, k_2)$ denote the 2D DFTs of the two images. $F(k_1, k_2)$ is given by

$$\begin{aligned} F(k_1, k_2) &= \sum_{n_1, n_2} f(n_1, n_2) W_{N_1}^{k_1 n_1} W_{N_2}^{k_2 n_2} \\ &= A_F(k_1, k_2) e^{j\theta_F(k_1, k_2)}, \end{aligned} \quad (1)$$

where $k_1 = -M_1, \dots, M_1$, $k_2 = -M_2, \dots, M_2$, $W_{N_1} = e^{-j\frac{2\pi}{N_1}}$, $W_{N_2} = e^{-j\frac{2\pi}{N_2}}$, and \sum_{n_1, n_2} denotes $\sum_{n_1=-M_1}^{M_1} \sum_{n_2=-M_2}^{M_2}$. $A_F(k_1, k_2)$ is amplitude and $\theta_F(k_1, k_2)$ is phase. $G(k_1, k_2)$ is defined in the same way. The cross-phase spectrum $R_{FG}(k_1, k_2)$ is given by

$$R_{FG}(k_1, k_2) = \frac{F(k_1, k_2) \overline{G(k_1, k_2)}}{|F(k_1, k_2) \overline{G(k_1, k_2)}|} = e^{j\theta(k_1, k_2)}, \quad (2)$$

where $\overline{G(k_1, k_2)}$ is the complex conjugate of $G(k_1, k_2)$ and $\theta(k_1, k_2)$ denotes the phase difference $\theta_F(k_1, k_2) - \theta_G(k_1, k_2)$.

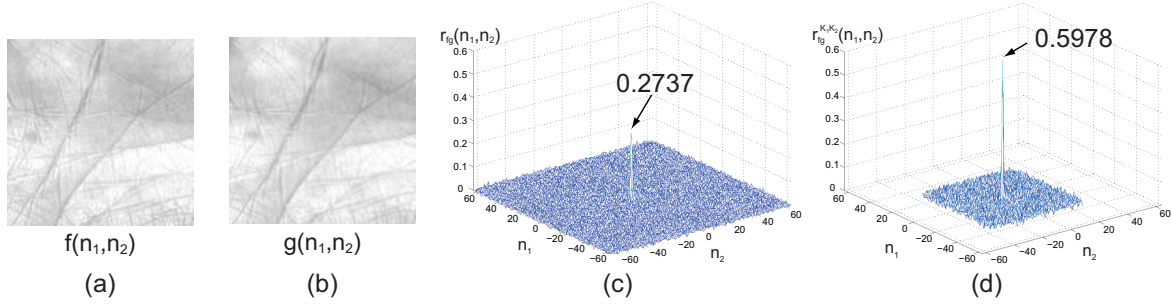


Fig. 1. Example of genuine matching using the original POC function and the BLPOC function: (a) registered palmprint image $f(n_1, n_2)$, (b) input palmprint image $g(n_1, n_2)$, (c) original POC function $r_{fg}(n_1, n_2)$ and (d) BLPOC function $r_{fg}^{K_1 K_2}(n_1, n_2)$ with $K_1/M_1 = 0.5$ and $K_2/M_2 = 0.5$.

The POC function $r_{fg}(n_1, n_2)$ is the 2D Inverse DFT (2D IDFT) of $R_{FG}(k_1, k_2)$ and is given by

$$r_{fg}(n_1, n_2) = \frac{1}{N_1 N_2} \sum_{k_1, k_2} R_{FG}(k_1, k_2) W_{N_1}^{-k_1 n_1} W_{N_2}^{-k_2 n_2}, \quad (3)$$

where \sum_{k_1, k_2} denotes $\sum_{k_1=-M_1}^{M_1} \sum_{k_2=-M_2}^{M_2}$. When two images are similar, their POC function gives a distinct sharp peak. When two images are not similar, the peak drops significantly. The height of the peak gives a good similarity measure for image matching, and the location of the peak shows the translational displacement between the images.

We modify the definition of POC function to have a BLPOC (Band-Limited Phase-Only Correlation) function [5] dedicated to palmprint matching tasks. The idea to improve the matching performance is to eliminate meaningless high frequency components in the calculation of cross-phase spectrum R_{FG} depending on the inherent frequency components of palmprint images. Assume that the ranges of the inherent frequency band are given by $k_1 = -K_1, \dots, K_1$ and $k_2 = -K_2, \dots, K_2$, where $0 \leq K_1 \leq M_1$ and $0 \leq K_2 \leq M_2$. Thus, the effective size of frequency spectrum is given by $L_1 = 2K_1 + 1$ and $L_2 = 2K_2 + 1$. The BLPOC function is given by

$$r_{fg}^{K_1 K_2}(n_1, n_2) = \frac{1}{L_1 L_2} \sum'_{k_1, k_2} R_{FG}(k_1, k_2) W_{L_1}^{-k_1 n_1} W_{L_2}^{-k_2 n_2}, \quad (4)$$

where $n_1 = -K_1, \dots, K_1$, $n_2 = -K_2, \dots, K_2$, and \sum'_{k_1, k_2} denotes $\sum_{k_1=-K_1}^{K_1} \sum_{k_2=-K_2}^{K_2}$. Note that the maximum value of the correlation peak of the BLPOC function is always normalized to 1 and does not depend on L_1 and L_2 .

Figure 1 shows an example of genuine matching using the original POC function r_{fg} and the BLPOC function $r_{fg}^{K_1 K_2}$. The BLPOC function provides the higher correlation peak and better discrimination capability than that of the original POC function.

3. PALMPRINT RECOGNITION ALGORITHM

In this section, we present a palmprint recognition algorithm using the POC function. The proposed algorithm consists of

the three steps: (i) rotation and displacement alignment, (ii) common region extraction and (iii) palmprint matching.

(i) Rotation and displacement alignment

We need to normalize rotation and displacement between the registered image $f(n_1, n_2)$ and the input image $g(n_1, n_2)$ in order to perform the high-accuracy palmprint matching.

At first, we reduce the effect of background components in palmprint images by applying 2D spatial window to the two images $f(n_1, n_2)$ and $g(n_1, n_2)$. The 2D Hanning window is applied at the center of gravity of each palmprint to align rotation and displacement between the two images $f(n_1, n_2)$ and $g(n_1, n_2)$ correctly. The center of gravity of each palmprint is detected by using n_1 -axis projection and n_2 -axis projection of pixel values. Figure 2 (a) shows the palmprint images and their centers of gravity, and (b) shows the palmprint images, $f_w(n_1, n_2)$ and $g_w(n_1, n_2)$, after applying 2D Hanning window.

Next, we estimate the rotation angle θ using the amplitude spectra of $f_w(n_1, n_2)$ and $g_w(n_1, n_2)$ as follows (see [4] for detailed discussions).

1. Calculate 2D DFTs of $f_w(n_1, n_2)$ and $g_w(n_1, n_2)$ to obtain $F_w(k_1, k_2)$ and $G_w(k_1, k_2)$.
2. Calculate amplitude spectra $|F_w(k_1, k_2)|$ and $|G_w(k_1, k_2)|$.
3. Calculate the polar mappings $|F_P(l_1, l_2)|$ and $|G_P(l_1, l_2)|$.
4. Estimate the image displacement between $|F_P(l_1, l_2)|$ and $|G_P(l_1, l_2)|$ using the peak location of the BLPOC function $r_{|F_P||G_P|}^{K_1 K_2}(n_1, n_2)$ to obtain θ .

Using θ , we obtain a rotation-normalized image $g_{w\theta}(n_1, n_2)$. Then, we align the translational displacement between $f_w(n_1, n_2)$ and $g_{w\theta}(n_1, n_2)$ using the peak location of the BLPOC function $r_{f_w g_{w\theta}}^{K_1 K_2}(n_1, n_2)$. Thus, we have normalized versions of the registered image and the input image as shown in Fig. 2 (c), which are denoted by $f'(n_1, n_2)$ and $g'(n_1, n_2)$.

(ii) Common region extraction

Next step is to extract the overlapped region (intersection) of the two images $f'(n_1, n_2)$ and $g'(n_1, n_2)$. This process improves the accuracy of palmprint matching, since the non-overlapped areas of the two images become the uncorrelated noise components in the BLPOC function. In order

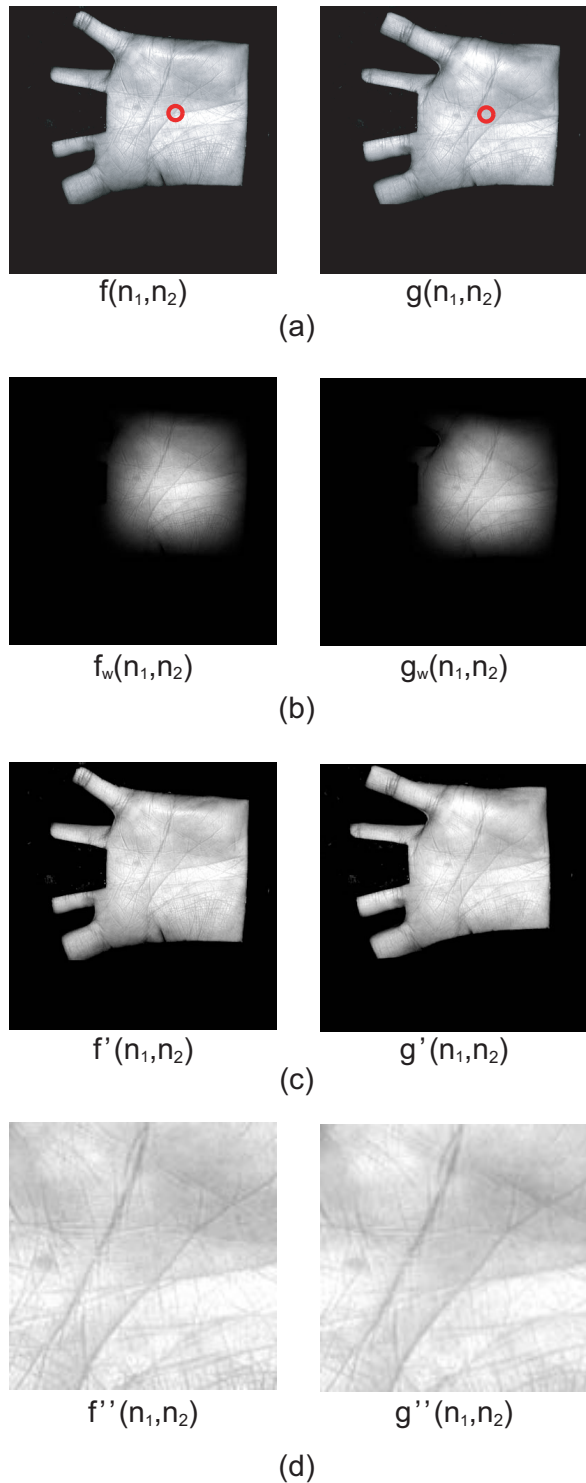


Fig. 2. Rotation and displacement alignment and common region extraction: (a) the registered image $f(n_1, n_2)$, the input image $g(n_1, n_2)$, (b) images, $f_w(n_1, n_2)$ and $g_w(n_1, n_2)$, after applying 2D Hanning window, (c) normalized images $f'(n_1, n_2)$ and $g'(n_1, n_2)$, and (d) extracted common regions $f''(n_1, n_2)$ and $g''(n_1, n_2)$.

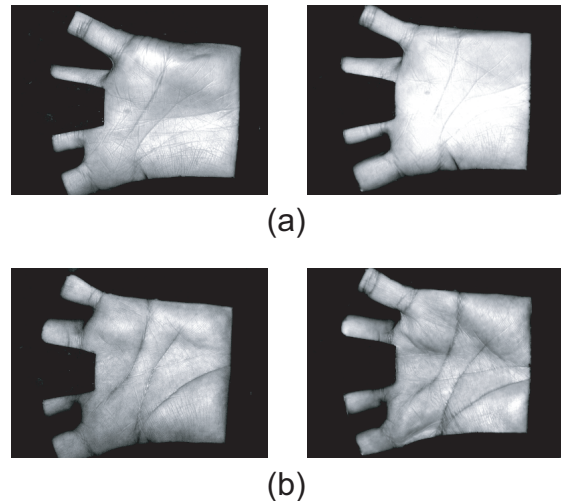


Fig. 3. Examples of palmprint images in the PolyU palmprint database: palmprint image pairs with different lighting condition (a) and nonlinear distortion (b).

to detect the effective palmprint areas in the registered image $f'(n_1, n_2)$ and the input image $g'(n_1, n_2)$, we examine the n_1 -axis projection and the n_2 -axis projection of pixel values. Only the common effective image areas, $f''(n_1, n_2)$ and $g''(n_1, n_2)$, with the same size are extracted for the succeeding image matching step (Fig. 2 (d)).

(iii) Palmprint matching

We calculate the BLPOC function $r_{f''g''}^{K_1K_2}(n_1, n_2)$ between the two extracted images $f''(n_1, n_2)$ and $g''(n_1, n_2)$, and evaluate the matching score. The matching score is the highest peak value of the BLPOC function $r_{f''g''}^{K_1K_2}(n_1, n_2)$.

4. EXPERIMENTAL RESULTS

This section describes a set of experiments using the PolyU palmprint database [10] for evaluating palmprint matching performance of the proposed algorithm. This database consists of 600 images (384×284 pixels) with 100 subjects and 6 different images of each palmprint. Figure 3 shows some examples of palmprint images in this database.

The performance of the biometrics-based identification system is evaluated by the Receiver Operating Characteristic (ROC) curve, which illustrates the Genuine Acceptance Rate (GAR) against the False Acceptance Rate (FAR) at different thresholds on the matching score. We first evaluate the GAR for all possible combinations of genuine attempts; the number of attempts is ${}_6C_2 \times 100 = 1500$. Next, we evaluate the FAR for ${}_{100}C_2 = 4950$ impostor attempts, where we select a single image (the first image) for each palmprint and make all the possible combinations of impostor attempts. The performance is also evaluated by the Equal Error Rate (EER), which is defined as the error rate where $100 - \text{GAR} = \text{FAR}$.

We consider reducing the computation time while optimizing the matching performance of the proposed algorithm

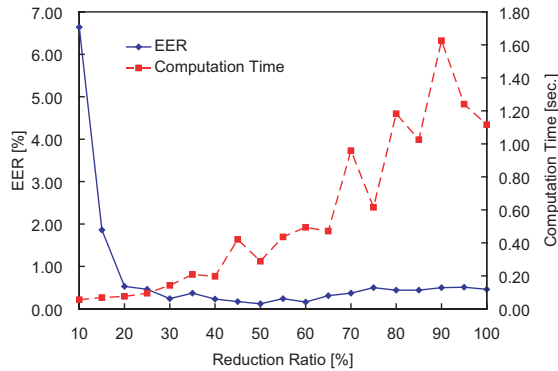


Fig. 4. EER and computation time against the image size reduction.

by changing the palmprint image size and the bandwidth parameters of BLPOC function K_1/M_1 and K_2/M_2 , respectively. In our previous work on phase-based fingerprint recognition [7], we can reduce the image size without considerable degradation of matching performance. We expect that the similar tendency is observed in the phase-based palmprint recognition. Figure 4 plots EER and computation time of the proposed algorithm when changing the image reduction ratio, where the parameters K_1/M_1 and K_2/M_2 are optimized for every point. The image reduction ratio is changed from 10% to 100%, and the parameters K_1/M_1 and K_2/M_2 are changed from 0.05 to 1.00. The computation time is evaluated by using MATLAB 6.5.1 on Pentium4 3.2 GHz. As a result, the optimal performance is observed when the image reduction ratio is 50% and $K_1/M_1 = K_2/M_2 = 0.75$. In this case, the EER of the proposed algorithm is 0.12% and the computation time is 0.29 seconds.

We compare two different matching algorithms: (A) a feature-based algorithm [2] and (B) the proposed algorithm. Figure 5 shows the ROC curves for the two algorithms. The proposed algorithm (B) exhibits significantly higher performance, since its ROC curve is located at higher GAR and lower FAR region than that of the feature-based algorithm (A). The EER of the proposed algorithm (B) is 0.12%, while the EER of the feature-based algorithm (A) is 0.45%. As is observed in the above experiments, the proposed algorithm is particularly useful for verifying low-quality palmprint images.

5. CONCLUSION

This paper proposed a palmprint recognition algorithm using the phase-based image matching. Experimental performance evaluation demonstrates an efficient performance of our proposed algorithm compared with the feature-based algorithm.

We have already demonstrated that the phase-based image matching is also effective for fingerprint and iris recognition tasks. Hence, we can expect that the proposed approach may be useful for multimodal biometric system having palmprint, fingerprint and iris recognition capabilities.

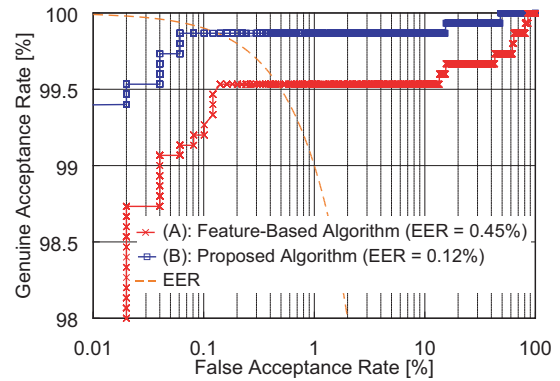


Fig. 5. ROC curves and EERs.

6. ACKNOWLEDGMENT

Portions of the research in this paper use the PolyU palmprint database collected by Hong Kong Polytechnic University.

7. REFERENCES

- [1] D. Zhang, *Palmprint Authentication*. Kluwer Academic Publication, 2004.
- [2] D. Zhang, W.-K. Kong, J. You, and M. Wong, "Online palmprint identification," *IEEE Trans. Pattern Anal. Machine Intell.*, vol. 25, no. 9, pp. 1041–1050, Sept. 2003.
- [3] C. D. Kuglin and D. C. Hines, "The phase correlation image alignment method," *Proc. Int. Conf. Cybernetics and Society*, pp. 163–165, 1975.
- [4] K. Takita, T. Aoki, Y. Sasaki, T. Higuchi, and K. Kobayashi, "High-accuracy subpixel image registration based on phase-only correlation," *IEICE Trans. Fundamentals*, vol. E86-A, no. 8, pp. 1925–1934, Aug. 2003.
- [5] K. Ito, H. Nakajima, K. Kobayashi, T. Aoki, and T. Higuchi, "A fingerprint matching algorithm using phase-only correlation," *IEICE Trans. Fundamentals*, vol. E87-A, no. 3, pp. 682–691, Mar. 2004.
- [6] K. Ito, A. Morita, T. Aoki, T. Higuchi, H. Nakajima, and K. Kobayashi, "A fingerprint recognition algorithm combining phase-based image matching and feature-based matching," *Lecture Notes in Computer Science (ICB2006)*, vol. 3832, pp. 316–325, Dec. 2005.
- [7] H. Nakajima, K. Kobayashi, M. Morikawa, A. Katsumata, K. Ito, T. Aoki, and T. Higuchi, "Fast and robust fingerprint identification algorithm and its application to residential access control products," *Lecture Notes in Computer Science (ICB2006)*, vol. 3832, pp. 326–333, Dec. 2005.
- [8] Products using phase-based image matching. [Online]. Available: <http://www.aoki.ecei.tohoku.ac.jp/research/poc.html>
- [9] K. Miyazawa, K. Ito, T. Aoki, K. Kobayashi, and H. Nakajima, "A phase-based iris recognition algorithm," *Lecture Notes in Computer Science (ICB2006)*, vol. 3832, pp. 356–365, Dec. 2005.
- [10] PolyU palmprint database. [Online]. Available: <http://www4.comp.polyu.edu.hk/biometrics/>
- [11] K. Takita, M. A. Muquit, T. Aoki, and T. Higuchi, "A subpixel correspondence search technique for computer vision applications," *IEICE Trans. Fundamentals*, vol. E87-A, no. 8, pp. 1913–1923, Aug. 2004.